

Ergodicity Test of the Eddy Correlation Method

Jinbei CHEN¹ Yinqiao HU² Ye YU Shihua LÜ

Key Laboratory of Land Surface Processes and Climate Change in Cold and Arid Regions; Cold and Arid Regions Environment and Engineering Institute, Chinese Academy of Sciences, Lanzhou 730000, P R China.

¹ E-mail: chenjinbei@lzb.ac.cn

² Corresponding author: hyq@ns.lzb.ac.cn

Abstract

The ergodic hypothesis is a basic hypothesis in atmospheric turbulent experiment. The ergodic theorem of the stationary random processes is introduced first into the turbulence in atmospheric surface layer (ASL) to analyze and verify the ergodicity of atmospheric turbulence measured by the eddy covariance system with two sets of field observational data of the ASL. The results show that eddies of atmospheric turbulence, of which the scale are smaller than the scale of atmospheric boundary layer (ABL), i.e. the spatial scale is less than 1,000 m and temporal scale is shorter than 10 min, can effectively satisfy the ergodic theorems. Therefore, the finite time average can be used to substitute for the ensemble average of atmospheric turbulence. Whereas, eddies are larger than ABL's scale, cannot satisfy the mean ergodic theorem. Consequently, when the finite time average is used to substitute for the ensemble average, a large rate of error would occurs with the eddy correction method due to the losing low frequency information of the larger eddies. The multi-station observation is compared with the single-station, and then the scope that satisfies the ergodic theorems is expanded from the smaller scale about 1000 m of ABL's scale to about 2000 m, even it exceeds ABL's scale. Therefore, the calculation of average, variance and fluxes of the turbulence can effectively satisfy the ergodic assumption, and the results are more approximate to the actual values. Regardless of vertical velocity or temperature, the variance of eddies in different scales can more efficiently follow MOST, if the ergodic theorem can be satisfied; or else it deviates from MOST. The exploration of ergodicity of the atmospheric turbulence is doubtlessly helpful to understanding the issues in atmospheric turbulent observation, and provides a theoretical basis for overcoming related difficulties.

Keywords: Ergodic hypothesis; eddy-correlation method; Monin-Obukhov similarity

34 theory (MOST); atmospheric surface layer (ASL); high-pass filtering

35

36 **1 Introduction**

37 The basic principle of average of the turbulence measurement is the ensemble average
38 of space, time and state. However, it is impossible that an actual turbulence
39 measurement with numerous observational instruments in space for enough time to
40 obtain all states of turbulent eddies to achieve the goal of ensemble average.
41 Therefore, based on the ergodic hypothesis, the time average of one spatial point,
42 which is long enough for observation, is used to substitute for the ensemble average
43 for temporally steady and spatially homogeneous surface (Stull 1988; Wyngaard 2010;
44 Aubinet 2012). The ergodic hypothesis is a basic assumption in atmospheric turbulent
45 experiment of the atmospheric boundary layer (ABL) and atmospheric surface layer
46 (ASL). The stationarity, homogeneity, and ergodicity are routinely used to link the
47 ensemble statistics (mean and higher-order moments) of field observational
48 experiments in the ABL. Many authors habitually refer to the ergodicity assumption,
49 as some descriptions such as “when satisfying ergodic hypothesis,

50 “something indicates that ergodic hypothesis is satisfied”. Though the success of
51 Monin-Obukhov similarity theory (MOST) for unstable and near-neutral conditions is
52 just an evidence of ergodic hypothesis validity in the ASL, however it is only a
53 necessary condition for ergodicity in the ASL experiments, does not proves ergodicity
54 (Katul et al., 2004). MOST success is under the conditions of stationary and
55 homogeneous surface. It implies that the stationarity and homogeneity are the
56 important conditions of ASL ergodicity. Therefore, many ABL’s experiments focus
57 on seeking ideal homogeneous surface as much as possible. And some test procedures
58 of availability are widely applied to establish stationarity (Foken and Wichura 1996;
59 Vickers and Mahrt 1997). Katul et al. (2004) qualitatively analyzed the ergodicity
60 problems in regarding atmospheric turbulence, and believed that it is common for the
61 neutral and unstable stratification in ASL to reach ergodicity, while it is difficult to
62 reach ergodicity for the stable layer. Eichinger et al. (2001) indicate that LIDAR
63 (Light Detection and Ranging) technique opens up new possibilities for atmospheric
64 measurements and analysis by providing spatial and temporal atmospheric
65 information with simultaneous high-resolution. The stationarity and ergodicity can be
66 tested for such ensembles of experiments. Recent advances in LIDAR measurements

67 offers a promising first step for direct evaluation of such hypotheses for ASL flows
68 (Higgins et al., 2013). Higgins et al. (2013) applied LIDAR of water vapor
69 concentration to investigate the ergodic hypothesis of atmospheric turbulence for the
70 first time. It is clear all the same that there is a need to reevaluate turbulence
71 measurement technology, to test the ergodicity of atmospheric turbulence
72 quantitatively by means of observation experiments.

73 The ergodic hypothesis was first proposed by Boltzmann (Boltzmann 1871; Uffink
74 2004) in his study of the ensemble theory of statistical dynamics. He argued that a
75 trajectory traverses *all* points on the energy hypersurface after a certain amount of
76 time. At the beginning of 20th century, Ehrenfest' couple proposed the quasi-ergodic
77 hypothesis and changed the term "traverses *all* points" in aforesaid ergodic hypothesis
78 to "passes arbitrarily close to every point". The basic points of ergodic hypothesis or
79 quasi-ergodic hypothesis recognize that the macroscopic property of system in the
80 equilibrium state is the average of microcosmic quantity in a certain amount of time.
81 Nevertheless, the ergodic hypothesis or quasi-ergodic hypothesis were never proven
82 theoretically. The proof of ergodic hypothesis in physics aroused the interest of
83 mathematicians. The famous mathematician, Neumann et al. (1932) first theoretically
84 proved the ergodic theorem in topological space (Birkhoff 1931, Krengel 1985).
85 Afterward, a banaisic ergodic theorem of stationary random processes was proved to
86 provide the necessary and sufficient conditions for the ergodicity of stationary random
87 processes. Mattingly (2003) reviewed the research progress of ergodicity of random
88 Navier-Stokes equations, and Galanti (Galanti et al. 2004, Lennaert et al. 2006) solved
89 the random Navier-Stokes equation by numerical simulation to prove that the
90 turbulence which is temporally steady and spatially homogeneous is ergodic.
91 However, Galanti (2004) also indicated that such partially turbulent flows acting as
92 mixed layer, wake flow, jet flow, flow around the boundary layer may be non-ergodic
93 turbulence.

94 Obviously, the advances of research on the ergodicity in the mathematics and
95 physics have precedence far over the atmospheric science. We try firstly to introduce
96 the ergodic theorem of stationary random processes to atmospheric turbulence in ASL
97 in this paper. And that the ergodicity of different scale eddies of atmospheric
98 turbulence is directly analyzed and verified quantitatively on the basis of the field
99 observational data measured by the eddy covariance system.

100 2 Theories and methods

101 2.1 Ergodic theorems of stationary random processes

102 The stationary random processes are the processes which will not vary with time, i.e.,
103 for observed quantity A , its function of spatial x_i and temporal t_i satisfies the following
104 condition:

$$105 A(x_1, x_2, \dots, x_n; t_1, t_2, \dots, t_n) = A(x_1, x_2, \dots, x_n; t_1 + \tau, t_2 + \tau, \dots, t_n + \tau), \quad (1)$$

106 where τ is a time period, defined as the relaxation time.

107 The mean μ_A of random variable A and autocorrelation function $R_A(\tau)$ are
108 respectively defined as follows:

$$109 \mu_A = \lim_{T \rightarrow +\infty} \frac{1}{T} \int_0^T A(t) dt, \quad (2)$$

$$110 R_A(\tau) = \lim_{T \rightarrow +\infty} \frac{1}{T} \int_0^T A(t) A(t + \tau) dt. \quad (3)$$

111 The autocorrelation function $R_A(\tau)$ is a temporal second-order moment. In the case of
112 $\tau=0$, the autocorrelation function $R_A(\tau)$ is the variance of random variable. The
113 necessary and sufficient conditions that stationary random processes satisfy the mean
114 ergodicity are the mean ergodic function $Ero(A)$ to zero (Papoulis et al. 1991), as
115 shown below:

$$116 Ero(A) = \lim_{T \rightarrow \infty} \frac{1}{T} \int_0^{2T} \left(1 - \frac{\tau}{2T}\right) [R_A(\tau) - \mu_A^2] d\tau = 0. \quad (4)$$

117 The mean ergodic function $Ero(A)$ is a time integral of variation between the
118 autocorrelation function $R_A(\tau)$ of variable A and its mean square, μ_A^2 . If the mean
119 ergodic function $Ero(A)$ converges to zero, then the stationary random processes will
120 be ergodic. In other words, if the autocorrelation function $R_A(\tau)$ of variable A
121 converges to its mean square, μ_A^2 , the stationary random processes are mean ergodic.

122 The Eq. (4) is namely the mean ergodic theorem to be called as well as ergodic
123 theorem of the weakly stationary processes in mathematics. For discrete variables, Eq.
124 (4) can be rewritten as the following:

$$125 Ero(A) = \lim_{n \rightarrow \infty} \sum_{i=0}^n \left(1 - \frac{\tau_i}{n}\right) [R_A(\tau_i) - \mu_A^2] = 0. \quad (5)$$

126 The Eq. (5) is the mean ergodic theorem of discrete variable. Hence, Eqs. (4) and (5)
127 can be used as a criterion to judge the mean ergodicity.

128 The necessary and sufficient conditions that stationary random processes satisfy the
 129 autocorrelation ergodicity are the autocorrelation ergodic function $\text{Er}(A)$ to zero:

$$130 \quad \text{Er}(A) = \lim_{T \rightarrow \infty} \frac{1}{T} \int_0^{2T} \left(1 - \frac{\tau'}{2T}\right) [B(\tau') - |R_A(\tau)|^2] d\tau' = 0; \quad (6a)$$

$$131 \quad B(\tau') = E \left\{ A(t + \tau + \tau') A(t + \tau') [A(t + \tau) A(t)] \right\}. \quad (6b)$$

132 where $B(\tau')$ is the temporal fourth-order moment of variable A . The autocorrelation
 133 ergodic function $\text{Er}(A)$ is a time integral of variation between the temporal
 134 fourth-order moment $B(\tau')$ of variable A and its autocorrelation function square,
 135 $|R_A(\tau)|^2$. If the autocorrelation ergodic function $\text{Er}(A)$ converges to zero, then the
 136 stationary random processes will be of autocorrelation ergodicity, and thus the
 137 autocorrelation ergodicity means that the fourth-order moment of variable of
 138 stationary random processes will converge to square of its autocorrelation function
 139 $R_A(\tau)$. The Eq. (6a) is namely the autocorrelation ergodic theorem to be called as well
 140 as the ergodic theorem of strongly stationary processes in the mathematics. The
 141 autocorrelation ergodic function of corresponding discrete variable can be determined
 142 as follows:

$$143 \quad \text{Er}(A) = \lim_{n \rightarrow \infty} \sum_{i=0}^n \left(1 - \frac{\tau'_i}{n}\right) [B(\tau'_i) - |R_A(\tau_j)|^2] = 0, \quad (7a)$$

$$144 \quad B(\tau'_i) = E \left\{ \sum_{j=0}^n A(t + \tau_j + \tau'_i) A(t + \tau'_i) [A(t + \tau_j) A(t)] \right\}. \quad (7b)$$

145 The Eq. (7a) is the autocorrelation ergodic theorem of discrete variable. Hence, Eqs.
 146 (6a) and (7a) can also be used as a criterion to judge autocorrelation ergodicity.

147 The stationary random processes conform to the criterion, Eqs. (4) or (5), viz.
 148 satisfy the mean ergodic theorem, or are intituled as the mean ergodicity; if the
 149 stationary random processes conform to Eqs. (6a) or (7a), then satisfy the
 150 autocorrelation ergodic theorem, or are intituled as the autocorrelation ergodicity. If
 151 the stationary random processes are only of mean ergodicity, then they are the strict
 152 ergodic or narrow ergodic. If the stationary random processes are of both the mean
 153 ergodicity and autocorrelation ergodicity, then they are the wide ergodic stationary
 154 random processes. It is thus clear that the ergodic random processes are stationary, but
 155 the stationary processes may not be ergodic.

156 With respect to the random process theory, when the mean and high-order moment
157 function is calculated, a large amount of repeated observations of random processes
158 require to acquire the sample function $A_k(t)$. If the stationary random processes satisfy
159 the ergodic conditions, then the time average of a sample on the whole time shaft can
160 be used to substitute for the overall or ensemble average. Eqs. (4), (5), (6a) and (7a)
161 can be used as the criterion to judge whether or not satisfying the mean and
162 autocorrelation ergodicity. The ergodic random processes must be the stationary
163 random processes to be defined as Eq. (1), and thus are stationary in relaxation time τ .
164 If conditions such as Eqs (4) and (5) of the mean ergodicity are satisfied, then a time
165 average in finite relaxation time τ can be used to substitute for the infinite time
166 average to calculate mean Eq. (2) of the random variable; similarly, the finite time
167 average can be used for substitution to calculate the covariance or variance of random
168 variable, Eq. (3), if conditions such as Eqs. (6a) and (7a) of autocorrelation ergodicity
169 are satisfied. In a similar manner, the basic principle of average of atmospheric
170 turbulence measurement is the ensemble average of space, time and state, and it is
171 necessary to carry through mass observation for a long period of time in the whole
172 space. This is not only a costly observation, even is hardly feasible. If the turbulence
173 signals satisfy the ergodic conditions, then the time average in relaxation time τ by
174 multi-station observation, even single-station observation, can substitute for the
175 ensemble average. In fact, the precondition to estimate the turbulent characteristic
176 quantities and fluxes in ABL by the eddy correlation method is that the turbulence
177 satisfies the ergodic conditions. Therefore, conditions such as Eqs. (4), (5), (6a) and
178 (7a) will also be the criterion for testing the authenticity of observed results by the
179 eddy correlation method.

180 **2.2 Band-pass filtering**

181 In the spatial scale, the atmospheric turbulence from the dissipation range, inertial
182 sub-range to energy range, and further large eddy of turbulent flow is extremely broad
183 (Stull 1988). Such spatial and temporal size of eddies include the isotropous 3-D eddy
184 structure of high frequency turbulence and orderly coherent structure of low
185 frequency turbulence (Li et al. 2002). The different scale eddies are also different in
186 terms of their spatial structure and physical properties, and even their transport
187 characteristics are not all the same. It is thus reasonable that eddies with different
188 transport characteristics are separated, processed and studied by using different

189 methods (Zuo et al. 2012). A major goal of our study is to understand what type of
 190 eddy in the scale can satisfy the ergodic conditions. Another goal is that the time
 191 averaging of signals measured by a single station determines accurately the turbulent
 192 characteristic quantities. In order to study the ergodicity of eddies in different scales,
 193 Fourier transform is used as band-pass filtering to distinguish the different scale
 194 eddies. That is to say, we set by the strong arm not needing part of frequencies as zero
 195 in the Fourier transform, and then acquire the signals after filtering by means of
 196 Fourier inverse transformation. The specific formulae are shown below:

$$197 \quad F_A(n) = \frac{1}{N} \sum_{k=0}^{N-1} A(k) \cos\left(\frac{2\pi nk}{N}\right) - \frac{i}{N} \sum_{k=0}^{N-1} A(k) \sin\left(\frac{2\pi nk}{N}\right), \quad (8)$$

$$198 \quad A(k) = \sum_{n=a}^{N-1} F_A(n) \cos\left(\frac{2\pi nk}{N}\right) + i^2 \sum_{n=a}^{N-1} F_A(n) \sin\left(\frac{2\pi nk}{N}\right). \quad (9)$$

199 In Eqs. (8) and (9), $F_A(n)$ and $A(k)$ are respectively the Fourier transformation and
 200 Fourier inverse transformation including N data points from $k=0$ to $k=N-1$, and n is the
 201 cycle index of the observation time range. The high-pass filtering can cut off the low
 202 frequency signals of turbulence to obtain high frequency signals. The aliasing of half
 203 high frequency turbulence after the Fourier transformation is unavoidable. At the
 204 same time, the correction for high frequency response will compensate for the loss. In
 205 order to acquire purely high frequency signals in the filtering processes, we take the
 206 results of band-pass filtering from $n=j$ to $n=N-j$ as the high frequency signals. This is
 207 referred to as j time filtering in this paper. Finally, the ergodicity of different scale
 208 eddies is analyzed using Eqs. (4)-(7).

209 **2.3 M-O similarity of turbulent variance**

210 The characteristics of relations of Monin-Obukhov similarity (MOS) of variance for
 211 the different scale eddies are analyzed and compared to test the feasibility of MOS's
 212 relation for the ergodic and non-ergodic turbulence. The problems of eddy correlation
 213 method in the turbulence observation in ASL are further explored on the basis of the
 214 study on the ergodicity and MOS's relations of the variance of different scale eddies
 215 in order to provide an experimental basis for utilizing MOST and developing the
 216 turbulence theory of ABL with complex underlying surfaces.

217 The MOS's relations of turbulent variance can be regarded as an effective
 218 instrumentality to verify whether or not the turbulent flow field is steady and
 219 homogeneous (Foken et al. 2004). Under ideal conditions, the local MOS's relations

220 of variance of wind velocity, temperature and other factors can be expressed as
 221 follows:

$$222 \quad \sigma_i/u_* = \phi_i(z/L), \quad (i = u, v, w), \quad (10)$$

$$223 \quad \sigma_s/|s_*| = \phi_s(z/L), \quad (s = \theta, q). \quad (11)$$

224 where σ is the turbulent variance; corner mark i is the wind velocity u , v or w ; s stands
 225 for scalar, such as potential temperature θ and humidity q ; u_* is the friction velocity

226 and defined as $u_* = \left(\overline{u'w'^2} + \overline{v'w'^2} \right)^{1/4}$; s_* is the turbulent characteristic quantity of

227 the related scalar and defined as $s_* = -\overline{w's'}/u_*$; and that M-O length L is defined as:

$$228 \quad L = u_*^2 \theta / [\kappa g (\theta_* + 0.61 \theta q_* / \rho_d)]. \quad (12)$$

229 A large number of research results show that, in the case of unstable stratification,
 230 $\phi_i(z/L)$ and $\phi_s(z/L)$ can be expressed in the following forms (Panofsky et al. 1977;
 231 Padro 1993; Katul et al. 1999):

$$232 \quad \phi_i(z/L) = c_1 (1 - c_2 z/L)^{1/3}; \quad (13)$$

$$233 \quad \phi_s(z/L) = \alpha_s (1 - \beta_s z/L)^{-1/3}. \quad (14)$$

234 where c_1 , c_2 , α and β are coefficients to be determined by the field observation. In the
 235 case of stable stratification, $\phi_s(z/L)$ is approximate to a constant and $\phi_i(z/L)$ is
 236 still the 1/3 function of z/L . The turbulent characteristics of eddies in the different
 237 temporal and spatial scales in are analyzed and compared with the mean and
 238 autocorrelation ergodic theorems, to test the feasibility of MOS's relations under
 239 conditions of the ergodic and non-ergodic turbulence.

240 3 The sources and processing of data

241 In this study, the first turbulence data that were measured by the eddy correlation
 242 method under the homogeneous surface in the Nagqu Station of Plateau Climate and
 243 Environment (NSPCE), Chinese Academy of Sciences (CAS) are used. The data set in
 244 NSPCE/CAS includes that measured by 3-D sonic anemometer and thermometer
 245 (CSAT3) with 10 Hz as well as infrared gas analyzer (Li7500) in ASL from 23 July
 246 2011 to 13 September 2011. In addition, the second turbulence data set of CASES-99
 247 (Poulos et al. 2002; Chang et al. 2002) is used to verify the ergodicity of turbulence

248 observed by multi-station. The data set is ASL's data in seven observation points. The
249 sub-towers, sn1, sn2 and sn3 are located 100 m away from the central tower, the sn4
250 is 280 m away, and tower sn5 and sn6 are located 300 m away. For CASES-99, the
251 data of sonic anemometer and thermometer (CSAT3) with 20 Hz and the infrared gas
252 analyzer (Li7500) in ASL at 10m on the central tower with 55 m height. And other
253 turbulence data include 3-D sonic anemometer (ATI) and Li7500 at 10 m height on
254 six sub-towers surrounding the central tower. The two sets of data collected for
255 completely different purposes are compared to test the universality of the research
256 results.

257 The geographic coordinate of NSPCE/CAS is 31.37°N, 91.90°E, and its altitude is
258 4509 m a.s.l. The observation station is built on flat and wide area except for a hill of
259 about 200 m at 2 km distance in the north, and floors area 8000m². The ground
260 surface is mainly composed of sandy soil mixed with sparse fine stones, and an alpine
261 meadow with vegetation of 10-20 cm. The displacement height of underlying surface
262 of NSPCE's meadow is determined to 0.03 m by calculation. CASES-99 is located in
263 prairie of Kansas US. The geographic coordinate of CASES-99's central tower is
264 37.65°N, 96.74°W. The observation field is flat and growth grasses about 20-50 cm
265 during the observation period, while the displacement height of the CASES-99's
266 underlying surface is 0.06 m (Martano 2002).

267 This study is conditioned to the stationary random processes. So the inaccurate
268 data in the measurements caused by circuit pulse are deleted before data analysis.
269 Subsequently, the data are divides into continuous sections of 5-hour, and the 1-hour
270 high frequency signals are obtained by applying filtering of Eqs. (8) and (9) on each
271 5-hour data. In order to conform to the stationary random condition and to select the
272 steady turbulent data, the 12 fragments of 5-min variances of the velocity and
273 temperature in 1-hour are calculated and compared with each other. When their
274 deviations are less than $\pm 15\%$ including an instrumental error about $\pm 5\%$, the data
275 are selected to study the ergodicity of the observed eddies. Moreover, the ultrasonic
276 temperature pulsation is corrected to absolute temperature pulsation (Schotanus et al.
277 1983; Kaimal et al. 1991). Then the coordinate is rotated using the plane fitting
278 method to improve the installation level (Wilczak 2001). The moisture is components
279 of the air; their pulsation is also a constituent part of the air density pulsation.
280 Therefore, there is no relevant correction on the humidity pulsation caused by air

281 density fluctuation. According to our preliminary analysis, such correlation may also
282 cause the unreason deviation from the prediction shown in Eq. (14). The Webb
283 correction (Webb et al. 1980) is the component of surface energy balance in physical
284 nature, but not the component of turbulent eddy. We thus do not perform Webb
285 correction on our research objectives of the ergodicity.

286 **4. Result analysis**

287 Applying the two sets of data from NSPCE and CASES-99, we have tested the
288 ergodicity of eddies in different temporal scales under the condition of steady
289 turbulence. Here, we carefully select the representative data measured at the level of
290 3.08m in NSPCE during three time frames, namely 3:00-4:00, 7:00-8:00 and
291 13:00-14:00 China Standard Time (CST) on 25 August in clear weather to test and
292 demonstrate the ergodicity of eddies in different temporal scales. These three time
293 frames can represent three situations, i.e. the nocturnal stable boundary layer, early
294 neutral boundary layer and midday convective boundary layer.

295 The trend correction (McMillen 1988; Moore 1986) is used to exclude the influence
296 of low-frequency trend effect. In order to acquire the effective information of eddies
297 in the different temporal scales, Eqs. (8) and (9) are used to perform band-pass
298 filtering of the turbulence data at 3.08 m in NSPCE, which is equivalent to the
299 correction of the high-pass filtering. In addition, the results of the time band-pass
300 filtering from $n=j$ to $n=N-j$ corresponding to Eqs. (8) and (9) acquire the information
301 of eddies in the corresponding temporal scale. The band-pass filtering information of
302 different time frames is thereby utilized to study the turbulence characteristics and
303 ergodicity of eddies in the different temporal scales of six time frames, including 2
304 min, 3 min, 5 min, 10 min, 30 min and 60 min.

305 **4.1 M-O eddy local stability and M-O stratification stability**

306 The M-O stratification stability z/L describe a whole characteristic between the
307 mechanical and buoyancy effects in ASL's turbulence, but this study will decompose
308 the turbulence into the different scale eddies. Considering that the features of different
309 scale eddies of the atmospheric turbulence varied with the atmospheric stability
310 parameter z/L , a M-O eddy local stability that is limited in the certain scale range of
311 eddies is defined as z/L_c , so as to analyze the relation between the stratification
312 stability and ergodicity of the wind velocity, temperature and other factors of the
313 different scale eddies. It is noted that the M-O eddy local stability, z/L_c , is different

314 from the M-O stratification stability, z/L .

315 As an example, the eddy local stability z/L_c in the different temporal scales of the
316 three time frames from nighttime to daytime is as shown in Table 1. The results show
317 that the eddy local stability z/L_c below 2 min in temporal scale during the nighttime
318 time frame of 3:00-4:00 is 0.59, thus it is stable stratification. For the eddies of which
319 the temporal scale gradually increases from 3 min, 5 min and 10 min to 60 min, but
320 the eddy local stability, z/L_c , gradually decreases to 0.31 and 0.28. In addition,
321 beginning from eddies of 10 min in the temporal scale, even the eddy local stability
322 decreases from -0.01 to -0.07. It seems that the eddy local stability gradually varies
323 from stable to unstable as the eddy temporal scale increases. During the morning time
324 frame of 7:00-8:00, the eddy local stability z/L_c from 2 min to 60 min in the temporal
325 scale eventually decreases from 0.52, 0.38, 0.16 and 0.15 to a minimum of -1.29. It
326 means that eddies in the temporal scales of 30 min and 60 min have high local
327 instability. However, during the midday time frame of 14:00-15:00, eddies in the
328 temporal scales from 2 min to 60 min are unstable. As the eddy scale increases, the
329 local instability of eddies in the scales from 2 min to 3 min also increases, and the
330 instability value reaches the maximum of 0.44 when the eddy scale is 5 min; the eddy
331 scale continuously increases, but the eddy local instability decreases.

332 The M-O eddy local stability is not entirely the same as the M-O stratification
333 stability of ABL in the physical significance. The M-O stratification stability of ABL
334 indicates that the overall effect of atmospheric stratification of the ABL on the
335 stability including all eddies in integral boundary layer. The M-O stratification
336 stability z/L of the no filtering data to include the whole turbulent signals is stable
337 0.02 for 3:00-4:00 (CST), but unstable -0.004 and -0.54 for 7:00-8:00 and
338 13:00-14:00 (CST), respectively. But the eddy local stability is only a local effect of
339 atmospheric stratification on the stability of eddies in a certain scale. As the eddy
340 scale increases, the eddy local stability z/L_c will vary accordingly. The aforesaid
341 results indicate that the local stability of small-scale eddies is stable in the nocturnal
342 stable boundary layer, but the nocturnal stable boundary layer is possibly unstable for
343 the large-scale eddies, so to result in a sink effect on the small-scale eddies, but a
344 positive buoyancy effect on the large-scale eddies. However, in the diurnal unstable
345 boundary layer, the eddy local stability of 3 min scale reaches the maximum, than
346 which the instability of smaller scale eddy decreases. But the instability gradually also

347 decreases as the eddy scale increases. Therefore, eddies of 3 min scale hold maximum
348 buoyancy, but the eddy buoyancy decreases as the eddy scale increases. However, the
349 small-scale eddies are more stable than eddies in the large scale in the nocturnal stable
350 boundary layer; while the large-scale eddies are more stable than the eddies in the
351 small scales in the diurnal unstable and convective boundary layers. The above facts
352 signify that it is common that there exist mainly the small-scale eddies in the
353 nocturnal boundary layer with stable stratification. And it is also common that there
354 exist mainly the large-scale eddies in the diurnal convective boundary layer with
355 unstable stratification. Therefore, it can well understand that the small-scale eddies are
356 dominant in the nocturnal stable boundary layer, while the large-scale eddies are
357 dominant in the diurnal convective boundary layer.

358 **4.2 Verification of mean ergodic theorem of eddies in different temporal scales**

359 In order to verify the mean ergodic theorem, we calculated the mean and
360 autocorrelation functions using Eq. (2) and Eq. (3), then calculated the variation of
361 mean ergodic function $Ero(A)$ using Eq. (5) of eddies in the different temporal scales
362 with relaxation time τ to be cut off with $\tau_{i=n}$. The mean ergodic functions, $Ero(A)$, of
363 vertical velocity, temperature and specific humidity of the different scale eddies are
364 calculated by using the data at level of 3.08m for the three time frames of 3:00-4:00,
365 7:00-8:00 and 13:00-14:00 (CST) in NSPCE, as shown in Figs. 1-3 respectively. Since
366 the ergodic function varies within a large range, the ergodic functions are normalized
367 according to the characteristic quantity of relevant variables ($A_* = u_*, |\theta_*|, |q_*|$). That is
368 to say, the functions in all following figures are dimensionless ergodic functions,
369 $Ero(A)/A_*$.

370 The comprehensive analyses of the mean ergodicity characteristics of atmospheric
371 turbulence and the relevant causes:

372 4.2.1 Verifying mean ergodic theorem of different scale eddies

373 According to the mean ergodic theorem, Eq. (4), the mean ergodic function $Ero(A)/A_*$
374 will converge to 0 if the time approaches infinite. This is a theoretical result of the
375 stationary random processes. However, the practical mean ergodic function is
376 calculated under the condition of that relaxation time $\tau_{i=n}$ is cut off. If the mean
377 ergodic function $Ero(A)/A_*$ verges approximately to 0 in relaxation time $\tau_{i=n}$, it will be
378 considered that random variable A approximately satisfies the mean ergodic theorem.
379 The mean ergodic function deviates more from zero, the mean ergodicity will be of

380 poor quality. So as we can judge approximately whether or not the mean ergodic
381 theorem of eddies in different scales holds. Figs. 1-3 clearly show that, regardless of
382 the vertical velocity, temperature or humidity, the $Ero(A)/A^*$ of eddies below 10 min in
383 the temporal scale will swing around zero within a small range; thus we can conclude
384 that the mean ergodic function $Ero(A)/A^*$ of eddies below 10 min in the temporal scale
385 converges to zero to satisfy effectively the conditions of mean ergodic theorem. For
386 eddies of 30 min and 60 min, which are larger scale, then the mean ergodic function
387 $Ero(A)/A^*$ will deviate further from zero. In particular, the mean ergodic function
388 $Ero(A)/A^*$ of eddies of 30 min and 60 min of the temperature or humidity does not
389 converge, and even diverges. The above results show that the mean ergodic function
390 of eddies of 30 min and 60 min cannot converge to zero or cannot satisfy the
391 conditions of mean ergodic theorem.

392 4.2.2 Comparison of the convergence of mean ergodic functions of vertical velocity, 393 temperature and humidity

394 As seen from Figs. 1-3, the dimensionless mean ergodic function of the vertical
395 velocity is compared with the respective function of the temperature and humidity, it
396 is 3-4 magnitudes less than those in the nocturnal stable boundary layer; 1-2
397 magnitudes less than those in the early neutral boundary layer; and around 2
398 magnitudes less than those in the midday convective boundary layer. For example,
399 during nighttime time frame of 3:00-4:00 (CST), the dimensionless mean ergodic
400 function of vertical velocity is 10^{-5} in magnitude, while the respective magnitudes of
401 function value of the temperature and humidity are 10^{-1} and 10^{-2} ; during morning time
402 frame of 7:00-8:00 (CAT), the magnitude of mean ergodic function of the vertical
403 velocity is 10^{-4} , while the respective magnitudes of function value of the temperature
404 and humidity are 10^{-2} and 10^{-3} ; during midday time frame of 13:00-14:00 (CST), the
405 magnitude of mean ergodic function of the vertical velocity is 10^{-4} , while the
406 magnitudes of function value of the temperature and humidity are both 10^{-2} . These
407 results show that the dimensionless mean ergodic function of vertical velocity
408 converges to zero much more easily than respective function value of the temperature
409 and humidity, and that the vertical velocity satisfies the conditions of mean ergodic
410 theorem more easily than the temperature and humidity.

411 4.2.3 Temporal scale and spatial scale of turbulent eddy

412 For wind velocity of $1-2 \text{ ms}^{-1}$, the eddy spatial scale in the temporal scale 2 min is

413 around 120-240 m, and the eddy spatial scale in the temporal scale 10 min is around
414 600-1200 m. The eddy spatial scale in the temporal scale 2 min is equivalent to the
415 ASL's height, and the eddy spatial scale in the temporal scale 10 min is equivalent to
416 ABL's height. The eddy spatial scale within the temporal scale 30-60 min is around
417 1800-3600 m, and this spatial scale clearly exceeds ABL's height to belong to the
418 scope of atmospheric local circulation. According to the stationary random processes
419 definition (1) and the mean ergodic theorem, the stationary random processes must be
420 smooth in the relaxation time τ . The eddies below temporal scale 10 min, i.e. below
421 ABL's height are the stationary random processes, and can effectively satisfy the
422 conditions of mean ergodic theorem. However, eddies in the temporal scale 30 min
423 and 60 min exceed the ABL's height do not satisfy the conditions of mean ergodic
424 theorem, thus these eddies belong to the non-stationary random processes.

425 4.2.4 Ergodicity of the turbulence of all eddies of possible scale in ABL

426 To facilitate comparison, Fig. 4 shows the variation of mean ergodic function $Ero(A)$
427 of the vertical velocity (a), temperature (b) and specific humidity (c) before filtering
428 with relaxation time τ during midday 14:00-15:00 (CST) in the convective boundary
429 layer. It is obvious that Fig. 4 is unfiltered mean ergodic function of eddies in all
430 possible scale in ABL. The Fig. 4 compares with Figs. 1c, 2c and 3c, which are the
431 mean ergodic function $Ero(A)/A^*$ of vertical velocity, temperature and humidity after
432 filtering during the midday time frame of 14:00-15:00 (CST). The result shows that
433 the mean ergodic functions before filtering are greater than that after filtering. As
434 shown in Figs. 1c, 2c and 3c, the magnitude for the vertical velocity is 10^{-4} and the
435 magnitudes for the temperature and specific humidity are both 10^{-2} . According to Fig.
436 4, the magnitude of vertical velocity $Ero(A)/A^*$ is 10^{-3} and the magnitudes of
437 temperature and specific humidity are both 10^0 , therefore 1-2 magnitudes are almost
438 decreased after filtering. Moreover, all trend upward for vertical velocity and
439 temperature and downward for specific humidity, deviating from zero. It is thus clear
440 that, even if the midday 14:00-15:00 (CST). when is equivalent to local time
441 12:00-13:00, the mean ergodic function of eddies in all possible scale in the
442 convective boundary layer cannot converge to zero before filtering, i.e. cannot satisfy
443 the conditions of mean ergodic theorem. That may be that eddies in all possible scale
444 before filtering including the local circulation in convective boundary layer. So we
445 argue that, under general situations, the eddies only below 10 min in the temporal

446 scale or within 600-1200 m in the spatial scale in ABL are the ergodic stationary
447 random processes, but the turbulence including the eddies with all possible scale in
448 ABL may belong to the non-ergodic stationary random processes.

449 4.2.5 Relation between the ergodicity and local stability of different scale eddies

450 The corresponding eddy local stability z/L_c of eddies at different times in different
451 scales (see Table 1) show that the eddy local stability z/L_c of the different scale eddies
452 are different, due to the fact that the temperature stratification in ABL has different
453 effects on the stability of in the different scale eddies. Even entirely contrary results
454 can occur. At the same time the stratification which can cause the large scale eddy to
455 ascend with buoyancy may cause the small scale eddy to descend. However, the
456 analysis results in Figs. 1-3 show that the ergodicity is mainly related to the eddy
457 scale, and its relation with the atmospheric temperature stratification seems
458 unimportance.

459 **4.3 Verification of autocorrelation ergodic theorem for different scale eddies**

460 In this section, Eqs. (7a) and (7b) are used to verify the autocorrelation ergodic
461 theorem. It is identified in Sect. 4.2 that the turbulent eddies below 10 min in the
462 temporal scale satisfy the mean ergodic conditions in the various time frames, i.e. the
463 turbulent eddies below 10 min in the temporal scale are at least in strictly stationary
464 random processes or narrow stationary random processes in the nocturnal stable
465 boundary layer, early neutral boundary layer and midday convective boundary layer.
466 Then we analyze further the different scale eddies which satisfy the mean ergodic
467 conditions whether or not also satisfy the autocorrelation ergodic conditions, so as to
468 verify whether atmospheric turbulence is in the narrow or wide stationary random
469 processes. The autocorrelation ergodic function of turbulence variable A under the
470 condition of truncated relaxation time $\tau_{i=n}$ are calculated according to Eq. (7a) to
471 determine the variation of autocorrelation ergodic function $Er(A)$ with relaxation time
472 τ . As with the mean ergodic function $Ero(A)$, if the autocorrelation ergodic function
473 $Er(A)$ of the eddies of 2 min, 3 min, 5 min, 10 min, 30 min and 60 min in the temporal
474 scale within the relaxation time $\tau_{i=n}$ is approximate to 0, then A shall be deemed to be
475 approximately ergodic; the more the autocorrelation ergodic function deviates from 0,
476 the worse the autocorrelation ergodicity becomes. Therefore, this method can be used
477 to judge approximatively whether the different scale eddies satisfy the conditions of
478 autocorrelation ergodic theorem.

479 For example, Fig. 5 shows the variation of normalized autocorrelation ergodic
480 function $Ero(w)/u_*$ of the turbulent eddies of 2 min, 3 min, 5 min, 10 min, 30 min and
481 60 min in the temporal scale with relaxation time τ for the vertical velocity during the
482 time frames of 3:00-4:00, 7:00-8:00 and 13:00-14:00 (CST). Some basic conclusions
483 are drawn from Fig. 5:

- 484 1. After comparing Figs. 5a-c with Figs. 1a-c, i.e. comparing the dimensionless mean
485 ergodic function $Ero(w)/u_*$ of vertical velocity with the dimensionless
486 autocorrelation ergodic function $Er(w)/u_*$, two basic characteristics are very clear.
487 First, the magnitudes of the dimensionless autocorrelation ergodic function
488 $Er(w)/u_*$, regardless of whether in the nocturnal stable boundary layer, early neutral
489 boundary layer or midday convective boundary layer, are all greatly reduced. In
490 Figs. 1a-c, the magnitudes of $Ero(w)/u_*$ are respectively 10^{-5} , 10^{-4} and 10^{-4} , and the
491 magnitudes of $Er(w)/u_*$ are respectively 10^{-7} , 10^{-5} and 10^{-5} , as shown in Figs. 5a-c.
492 The magnitudes of $Er(w)/u_*$ reduce by 1-2 magnitudes compared with those of
493 $Ero(w)/u_*$. Second, all autocorrelation ergodic functions $Er(w)/u_*$ of the eddies of
494 30 min and 60 min in temporal scale, regardless of whether they are in the stable
495 boundary layer, natural boundary layer or convective boundary layer, are all
496 reduced and approximate to $Ero(w)/u_*$ of the eddies below 10 min in temporal
497 scale.
- 498 2. The above two basic characteristics imply that the autocorrelation ergodic function
499 $Er(w)/u_*$ of the stable boundary layer, neutral boundary layer or convective
500 boundary layer converges to 0 faster than the mean ergodic function $Ero(w)/u_*$; the
501 autocorrelation ergodic function of eddies of 30 min and 60 min in temporal scale
502 also converges to 0 and satisfies the conditions of autocorrelation ergodic theorem,
503 except for the fact that the autocorrelation ergodic function $Er(w)/u_*$ of the eddies
504 below 10 min in temporal scale can converge to 0 and satisfy the conditions of
505 autocorrelation ergodic theorem.
- 506 3. According to the autocorrelation ergodic function Eq. (7a), the eddies of 30 min, 60
507 min and below 10 min in the temporal scale, regardless of whether they are in the
508 stable boundary layer, neutral boundary layer or convective boundary layer, all
509 eddies can satisfy the conditions of autocorrelation ergodic theorem. Therefore, in
510 general the ABL's turbulence is the stationary random processes of autocorrelation
511 ergodic.

512 4. The above results show that the eddies below 10 min in temporal scale in the
513 nocturnal stable boundary layer, early neutral boundary layer and midday
514 convective boundary layer can not only satisfy the conditions of mean ergodic
515 theorem, but also they can also satisfy the conditions of autocorrelation ergodic
516 theorem. Therefore, eddies below 10 min in the temporal scale are wide ergodic
517 stationary random processes. Although the eddies of 30 min and 60 min in
518 temporal scale in the stable boundary layer, neutral boundary layer and convective
519 boundary layer can satisfy the conditions of autocorrelation ergodic theorem, they
520 cannot satisfy the conditions of mean ergodic theorem. Therefore, eddies of 30 min
521 and 60 min in the temporal scale are neither narrow ergodic stationary random
522 processes, nor wide ergodic stationary random processes.

523 **4.4 Ergodic theorem verification of different scale eddies for the multiple stations**

524 The basic principle of turbulence average is the ensemble average of space, time and
525 state. Sections 4.2 and 4.3 verify the mean ergodic theorem and autocorrelation
526 ergodic theorem of atmospheric turbulence during the stationary random processes
527 using field observational data, so that the finite time average of a single station can be
528 used to substitute for the ensemble average. This section examines the ergodicity of
529 different scale eddies according to the observational data from the CASES-99 tower
530 and six sub-sites (seven stations). When the data are selected, it is considered that if
531 the eddies are not evenly distributed at the seven stations, then the observation results
532 at the seven stations may have originated from many eddies in the large scale. For this
533 reason, we first compared the high frequency variance spectrum above 0.1 Hz. Based
534 on the observational error, if the difference of all high frequency variances does not
535 exceed the average by $\pm 10\%$, then it is assumed that the turbulence is evenly
536 distributed at the seven observation stations. Finally, 17 datasets are chosen from
537 among the turbulence observation data from 5 to 30 October, and these data sets refer
538 to the results of strong turbulence at noon on a sunny day. As an example, the same
539 method as described in Sections 4.2 and 4.3 is used to respectively calculate the
540 variation of the mean ergodic function and the autocorrelation ergodic function of
541 vertical velocity in 10:00-11:00 on 7 October with relaxation time τ . Next, the
542 observation data chosen from the seven stations are built into a data set, and the time
543 series of data set are filtered at 2 min, 3 min, 5 min, 10 min, 30 min and 60 min. The
544 variations of mean ergodic function $Ero(w)/u_*$ and autocorrelation ergodic function

545 $Er(w)/u^*$ of the vertical velocity with relaxation time τ are analyzed to test the
546 ergodicity of different scale eddies for the observation of multi-station. Fig. 6a shows
547 the variation of mean ergodic function $Ero(w)/u^*$ of the vertical velocity with the
548 relaxation time τ , and Fig. 6b shows the variation of autocorrelation ergodic function
549 $Er(w)/u^*$ with the relaxation time τ .

550 The results show ergodic characteristics of different scale eddies measured at the
551 multi-stations as following:

552 Fig. 6a shows that the mean ergodic function of eddies below 30 min in temporal
553 scale converges to 0 very well, except for the fact that the mean ergodic function of
554 eddies of 60 min in temporal scale clearly deviates upward from 0. Fig. 6b shows that
555 all autocorrelation ergodic functions of different scale eddy, including eddies of 60
556 min in temporal scale, gradually converge to 0. Therefore, eddies below 30 min in
557 temporal scale measured at the multi-stations satisfy the conditions of both the mean
558 and autocorrelation ergodic theorems, while eddies of 60 min in temporal scale only
559 satisfies the conditions of autocorrelation ergodic theorem, but cannot satisfy the
560 conditions of mean ergodic theorem. These facts demonstrate that eddies below 30
561 min in temporal scale are wide ergodic stationary random processes in the data series
562 composed by the seven stations. This signifies that the comparing of data series
563 composed of multiple stations with data from a single station, the eddy temporal scale
564 for wide ergodic stationary random processes is extended from below 10 min to 30
565 min. As analyzed above, if the eddies below 10 min in temporal scale are deemed to
566 be the turbulent eddies in the ABL with height about 1000 m and the eddies of 30 min
567 in the temporal scale, which is equivalent to that the space scale is greater than 2000
568 m, are deemed including the eddy components of local circulation in ABL, then
569 multiple station observations can completely capture the local circulated eddies,
570 which space scale is greater than 2000 m.

571 **4.5 Average time problem of turbulent quantity averaging**

572 The atmospheric observations are impossible to repeat experiment exactly, must use
573 the ergodic hypothesis and replace ensemble averages with time averages. It arises a
574 problem how does determine the averaging time.

575 The analyses on the ergodicity of different scale eddies in above two sections
576 demonstrate that the eddies below 10 min in temporal scale as $\tau=30$ min in the stable
577 boundary layer, neutral boundary layer and convective boundary layer can not only

578 satisfy the conditions of mean ergodic theorem, but also can also satisfy the
579 conditions of autocorrelation ergodic theorem. That is to say, they are namely wide
580 ergodic stationary random processes. Therefore, the finite time average of 30 min
581 within relaxation time τ can be used for substituting for the ensemble average to
582 calculate mean random variable Eq. (2). However, the eddies of 30 min and 60 min in
583 the temporal scale in the stable boundary layer and neutral boundary layer are only
584 autocorrelation ergodic random processes, neither narrow nor wide sense random
585 processes. Therefore, when the finite time average of 30 min can be used for
586 substituting for the ensemble average to calculate mean random variable Eq. (2), it
587 may capture the eddies below 10 min in temporal scale in stationary random processes,
588 but not completely capture the eddies above 30 min in the temporal scale. The above
589 results signify that the turbulence average is restricted not only by the mean ergodic
590 theorem, but also is closely related to the scale of turbulent eddy. In the observation
591 performed using the eddy correlation method, the substitution of ensemble average
592 with finite time average of 30 min inevitably results in a high level of error, due to
593 lack of low frequency component information of the large-scale eddies. However,
594 although eddies of 30 min and 60 min in the temporal scale in convective boundary
595 layer are not wide ergodic stationary random processes, they are autocorrelation
596 ergodic random processes. This may imply that the mean random variable which is
597 calculated with the finite time average in the convective boundary layer to substitute
598 for the ensemble average is often superior to the results of the stable boundary layer
599 and neutral boundary layer. Withal, the results in the previous sections also show that
600 the mean ergodic function of vertical velocity may more easily converge to 0 than
601 functions corresponding to the temperature and humidity, and the vertical velocity
602 may more easily satisfy the conditions of mean ergodic theorem than the temperature
603 and humidity. Therefore, in the observation performed using the eddy correlation
604 method, the result of vertical velocity is often superior to those of the temperature and
605 humidity. In this section, the results also point out that multi-station observation is
606 cape of completely capturing eddies of local circumfluence in the ABL. Therefore, the
607 ergodic assumption is more likely to be satisfied, and its results are much closer to the
608 true values when calculating the turbulence mean, variance or fluxes with the
609 multi-station observation data.

610 In order to determine the averaging time, Oncley (1996) defined an Ogive function

611 of cumulative integral

$$612 \quad Og_{x,y}(f_0) = \int_{\infty}^{f_0} Co_{x,y}(f) df \quad (15)$$

613 where x and y are any two variables whose covariance is \overline{xy} , $Co_{xy}(f)$ is the
614 cospectrum of xy . If the Ogive function converges to a constant value at a frequency
615 $f=f_0$, which could be converted to the averaging time of the measurement. The Ogive
616 of $\overline{u'w'}$ is often examined to determine the least averaging time. As a comparison,
617 here the variation of Ogive functions of $\overline{w'^2}$ and $\overline{u'w'}$ with frequency at the height
618 3.08 m in NSPCE for the three time frames is shown in Fig.7. Fig.7 shows the
619 variation of Ogive convergence frequency for $\overline{w'^2}$ in the nighttime stable conditions,
620 morningtide neutral boundary layer and midday convection boundary layer converges
621 respectively converges about 0.01 Hz, 0.0001 Hz and 0.001 Hz. It is equivalent to the
622 averaging times about 2 min, 160 min and 16 min. However for $\overline{u'w'}$, it converges
623 about 0.001 Hz only in the midday convection boundary layer to be equivalent to the
624 averaging time about 16 min. However it seems no convergence in the nighttime
625 stable and morningtide neutral boundary layer. It is implied determining averaging
626 time seems to have a bit difficult with the Ogive function in the stable and neutral
627 boundary layer. The Fig.7 shows also that when the frequency is lower than 0.0001Hz,
628 Ogive functions $\overline{u'w'}$ ascend in the stable boundary layer, and descend in the
629 morningtide neutral boundary layer and midday convection boundary layer. It may be
630 low frequency effect caused the cross local circulation in the nighttime and midday in
631 ABL. Especially we must note that the Ogive is a function of the cumulative integral.
632 So as Ogive changes direction from ascending to descending, it implies that in the
633 negative momentum flux superimposing positive flux. The foremost reason that there
634 exists the positive up momentum flux at 3m level in the ASL is a local circulation
635 effect highly possible. The local circulation in ABL may be a cause that Ogive fails to
636 judge the averaging time. In this work, the choice of averaging time with the ergodic
637 theory seems superior to with the Ogive function.

638 **4.6 M-O similarity of turbulent eddies in different scales and its relation with** 639 **ergodicity**

640 Turbulent variance is a most basic characteristic quantity of the turbulence.
641 Turbulence velocity variance, which represents turbulence intensity, and the variance

642 of scalars, such as temperature and humidity, effectively describes the structural
 643 characteristics of turbulence. In order to test MOS relations of the different scale
 644 eddies with ergodicity, the vertical velocity and temperature data of NSPCE from 23
 645 July to 13 September are used to determine the MOS relationship of variances of
 646 vertical velocity and temperature for the different scale eddies, and analyze its relation
 647 with the ergodicity.

648 The MOS relation of vertical velocity variance as following:

$$649 \quad \phi_i(z/L) = c_1(1 - c_2 z/L)^{1/3}, \quad z/L < 0, \quad ,$$

650 (16)

$$651 \quad \phi_i(z/L) = c_1(1 + c_2 z/L)^{1/3}, \quad z/L > 0. \quad (17)$$

652 Fig. 8 and 9 respectively shows the MOS relation curves of different scale eddies for
 653 the vertical velocity and temperature variances in NSPCE. The figures (a), (b) and (c)
 654 of Fig. 8 and 9 are respectively the similarity curve of eddies of 10 min, 30 min and
 655 60 min in the temporal scale. Table 2 shows the relevant parameters of fitting curve of
 656 MOS relation for the vertical velocity variance. The correlation coefficient and
 657 residual of fitting curve are respectively expressed with R and S .

658 Fig. 8 and Table 2 show that the parameters of fitting curve are greatly different,
 659 even if the fitting curve modality of MOS relation of the vertical velocity variance for
 660 the eddies in different temporal scales is the same. The correlation coefficients of
 661 MOS's fitting curve of the vertical velocity variance under the unstable stratification
 662 are large, but the correlation coefficients under the stable stratification are small.
 663 Under unstable stratification, the correlation coefficient of eddies of 10 min in the
 664 temporal scale reaches 0.97, while the residual is only 0.16; under the stable
 665 stratification, the correlation coefficient reduces to 0.76, and the residual increases to
 666 0.25. With the increase of eddy temporal scale from 10 min (Fig. 8a) to 30 min (Fig.
 667 8b) and 60 min (Fig. 8c), the correlation coefficients of MOS relation of the vertical
 668 velocity variance gradually reduce, and the residual increases. The correlation
 669 coefficient in 60 min is the minimum; it is only 0.83 under the unstable stratification,
 670 and only 0.30 under the stable stratification.

671 The temperature variance is shown in Fig. 9. The MOS's function to fit from eddies
 672 of 10 min in the temporal scale under the unstable stratification is following:

$$673 \quad \phi_\theta(z/L_c) = 4.9(1 - 79.7 z/L_c)^{-1/3}. \quad (18)$$

674 As shown in Fig. 9a, the correlation coefficient of fitting curve is -0.91 and residual is
675 0.38. With the increase of eddy temporal scale, discreteness of MOS relation of the
676 temperature variance is enlarged quickly, and an appropriate curve cannot be fitted.

677 The above results show that the discreteness of fitting curve of MOS relation for
678 the turbulence variance is enlarged with the increase of eddy temporal scale for either
679 the vertical velocity or temperature. The points of data during the stationary processes
680 basically gather near the fitting curve of variance similarity relation, while all data
681 points during the nonstationary processes deviate significantly from the fitting curve.
682 However, the similarity of vertical velocity variance is superior to that of the
683 temperature variance. These results are consistent to the conclusions of testing
684 ergodicity for the different scale eddies described in Sections 4.2-4.4. The ergodicity
685 of small-scale eddy is superior to that of the larger-scale eddy, and eddies of 10 min in
686 the temporal scale has the best variance similarity function. These results also signify
687 that when the eddy at the stationary random processes satisfies the ergodic conditions,
688 then both the vertical velocity variance and temperature variance of eddies in the
689 different temporal scales comply with MOST very well; but, as for eddies with poor
690 ergodicity during nonstationary random processes, the variances deviate from MOS
691 relations.

692 **5 Conclusion**

693 From the above results, we can draw the below preliminary conclusions:

- 694 1. The turbulence in ABL is an eddy structure. When the temporal scale of turbulent
695 eddies in ABL is about 2 min, the corresponding spatial scale is about 120-240 m
696 to be equivalent to ASL's height; when the temporal scale of turbulent eddies in
697 ABL is about 10 min, the corresponding spatial scale is about 600-1200 m to be
698 equivalent to the ABL's height. As the larger temporal and spatial scale for eddies,
699 such as eddies of 30-60 min in the temporal scale, and the corresponding spatial
700 scale is about 1800-3600 m. Spatial scale exceeds the ABL's height.
- 701 2. For the atmospheric turbulent eddies below the ABL's scale, i.e. the eddies below
702 1000 m in the spatial scale and 10 min in the temporal scale, the mean ergodic
703 function $Ero(A)$ and autocorrelation ergodic function $Er(A)$ converge to 0, and they
704 can satisfy the conditions of mean and autocorrelation ergodic theorem. However,
705 for the atmospheric turbulent eddies above 2000-3000m in the spatial scale and
706 above 30-60 min in the temporal scale, the mean ergodic function doesn't converge

707 to 0, thus cannot satisfy the conditions of mean ergodic theorem. Therefore, the
708 turbulent eddies below the ABL's scale belong to the wide ergodic stationary
709 random processes, but the turbulent eddies which are larger than ABL's scale
710 belong to the non-ergodic random processes, or even the nonstationary random
711 processes.

712 3. Due to above facts, when the stationary random process information of eddies
713 below 10 min in the temporal scale and below 1000 m of ABL's height in the
714 spatial scale can be captured, the atmospheric turbulence may satisfy the conditions
715 of mean ergodic theorem. Therefore, an average of finite time can be used for
716 substituting for the ensemble average of infinite time to calculate mean random
717 variable as measuring atmospheric turbulence with the eddy correlation method.
718 But for the turbulence of eddies above 30 min in temporal scale and above 2000 m
719 in spatial scale magnitude, it cannot satisfy the conditions of mean ergodic theorem,
720 so that the eddy correlation method cannot completely capture the information of
721 nonstationary random processes. This will inevitably cause a high level of error
722 due to the lack of low frequency component information of the large-scale eddies
723 when the average of finite time is used to substitute for the ensemble average in
724 observation.

725 4. Although the atmospheric temperature stratification has different effects on the
726 stability of eddies in the different scales, the ergodicity is mainly related to the
727 local stability of eddies, and its relation with the stratification stability of ABL is
728 not significant.

729 5. The data series composed from seven stations compare with the observational data
730 from a single station. The results show that the temporal and spatial scale of eddies
731 to belong to the wide ergodic stationary random processes are extended from 10
732 min to below 30 min and from 1000 m to below 2000 m respectively. This signifies
733 that the ergodic assumption is more likely to be satisfied well with multi-station
734 observation data, and observational results produced by the eddy correlation
735 method are much closer to the true values when calculating the turbulence average,
736 variance or fluxes.

737 6. If the ergodic conditions of stationary random processes are more effectively
738 satisfied, then the turbulence variance of eddies in the different temporal scales
739 can comply with MOST very well; however, the turbulence variance of the

740 non-ergodic random processes deviates from MOS relations.

741

742 **6 Discussion**

743 1. Galanti (2004) proved that the turbulence which was temporally steady and
744 spatially homogeneous is ergodic, but ‘partially turbulent flows’ such as the mixed
745 layer, wake flow, jet flow, flow around and boundary layer flow may be
746 non-ergodic turbulence. However, it has been proven through atmospheric
747 observational data that the turbulence ergodicity is related to the scale of turbulent
748 eddies. Since the large-scale eddies in ABL may be strongly influenced by the
749 boundary disturbance, thus belong to ‘partial turbulence’; however, since the
750 small-scale eddies in atmospheric turbulence may be not influenced by boundary
751 disturbance, may be temporally steady and spatially homogeneous turbulence. So
752 that the mean ergodic theorem and autocorrelation ergodic theorem for the
753 turbulent eddies in small scale in ABL is applicative, but the large-scale eddies are
754 non-ergodic.

755 2. The eddy correlation method for turbulence measurement is based on the ergodic
756 assumption. A lack of ergodicity related to the presence of large-scale eddy
757 transport can lead to a consider error of a tower flux measurement. This has
758 already been pointed out by Mauder et al. (2007) or Foken et al. (2011). Therefore,
759 we realize from the above conclusions that the large scale eddies may include
760 non-ergodic random process components which exceed ABL’s height. The eddy
761 correlation method for the measurement and calculation of turbulent variance and
762 covariance may not capture the information of large-scale eddy exceeded ABL’s
763 scale, thus resulting in large error. MOST is developed on the conditions of steady
764 time and homogeneous surface. MOST’s conditions, steady time and homogeneous
765 surface, are in line with the ergodic conditions, therefore the turbulence variance,
766 even the turbulent fluxes of eddies in the different temporal scales may comply
767 with MOST very well, if the ergodic conditions of stationary random processes are
768 more effectively satisfied.

769 3. According to Kaimal and Wyngaard (1990), the atmospheric turbulence theory and
770 observation method were feasible and led to success under ideal conditions
771 including a short period, steady state and homogeneous underlying surface, and
772 through observation in the 1950s-1970s, but these conditions are rare in reality. In
773 the land surface processes and ecosystem, the turbulent flux observation in ASL is

774 a scientific issue in which commonly interest researchers in the fields of
775 atmospheric science, ecology, geography science, etc. These observations must be
776 implemented under conditions such as with complex terrain, heterogeneous surface,
777 long period and unsteady state. It is necessary that more neoteric observational
778 tools and theories will be applied with new perspectives in future research.

779 4. It is successful that the banausic ergodic theorem of stationary random processes is
780 introduced from the mathematics into atmospheric sciences. It undoubtedly
781 provides a profited tool for overcoming the challenges which encounter during the
782 modern measurement of atmospheric turbulent flow. At least it offers a promising
783 first step to diagnosticate directly the ergodic hypotheses for ASL's flows as a
784 criterion. And that the necessary and sufficient conditions of ergodic theorem can
785 introduce to the applicative scope of eddy correlation method and MOST, and seek
786 potential reasons disable for using them in the ABL.

787 5. In the future, we shall keep up to study the ergodic problems for the atmospheric
788 turbulence measurement under the conditions of complex terrain, heterogeneous
789 surface and unsteady, long observational period, and to seek effective schemes. The
790 above results indicate the atmospheric turbulent eddies below the scale of ABL can
791 be captured by the eddy correlation method and comply with MOST very well.
792 Perhaps MOST can be as the first order approximation to deal with the turbulence
793 of eddies below ABL's scale satisfying the ergodic theorems, then to compensate
794 the effects of eddies dissatisfying the ergodic theorems, which may be caused by
795 the advection, local circulation, low frequency effect, etc under the complex terrain,
796 heterogeneous surface. For example, we developed a turbulent theory of
797 non-equilibrium thermodynamics (Hu, Y., 2007; Hu, Y., et al., 2009) to find the
798 coupling effects of vertical velocity, which is caused by the advection, local
799 circulation, and low frequency, on the vertical fluxes. The coupling effects of
800 vertical velocity may be as a scheme to compensate the effects of eddies
801 dissatisfying the ergodic theorems (Hu, Y., 2003; Chen, J., et al., 2007, 2013).

802 6. It is clear that such studies are preliminary, and many problems require further
803 research. The attestation of more field experiments is necessary.

804

805 *Acknowledgements.* This study is supported by the National Natural Science
806 Foundation of China under Granted Nos. 91025011, 91437103 and National Program

807 on Key Basic Research Project (2010CB951701-2). This work was strongly supported
808 by Pingliang Land Surface Process & Severe Weather Research Station and the Heihe
809 Upstream Watershed Ecology-Hydrology Experimental Research Station, Chinese
810 Academy of Sciences. I would like to express my sincere regards for their support,
811 and also thank Dr. Gordon Maclean of NCAR for providing the detailed CASES-99
812 data used in this study. We thank referees very much for heartfelt comments,
813 discussion and marked errors of Referees.

814

815 References

816 Aubinet, M., Vesala, T., and Papale, D.: Eddy covariance, a practical guide to
817 measurement and data analysis, Springer, Dordrecht, Heidelberg, London, New
818 York, 438, 2012.

819 Birkhoff, G. D.: Proof of the ergodic theorem, Proc. Nat. Acad. Sci. USA. 18,
820 656-660, 1931.

821 Boltzmann, L.: Analytischer beweis des zweiten Hauptsatzes der mechanischen
822 Wärmetheorie aus den Sätzen über das Gleichgewicht der lebendigen Kraft, Wiener
823 Berichte , 63, 712-732, in WAI, paper 20, 1871.

824 Chang, S. S. and Huynh, G. D.: Analysis of sonic anemometer data from the
825 CASES-99 field experiment. Army Research Laboratory, Adelphi, MD. 2002.

826 Chen, J., Hu Y., and Zhang L.: Principle of cross coupling between vertical heat
827 turbulent transport and vertical velocity and determination of cross coupling
828 coefficient, Adv. Atmos. Sci., 23 (4), 639-648, 2007.

829 Chen, J., Hu, Y., Lu, S., and Yu, Ye.: Experimental demonstration of the coupling
830 effect of vertical velocity on latent heat flux, Sci. China. Ser. D-Earth Sci., 56,
831 1-9, 2013.

832 Eichinger, W. E., Parlange, M. B., Katul, G. G.: Lidar measurements of the
833 dimensionless humidity gradient in the unstable ASL, Lakshmi, V., Albertson, J.

834 and Schaake, J., Koster, R. D., Duan, Q., Land Surface Hydrology, Meteorology,
835 and Climate, American Geophysical Union, Washington, D. C. 7-13, 2001.

836 Foken, T., Wichura, B.: Tools for quality assessment of surface-based flux
837 measurements. *Agric For Meteorol.*, 78, 83-105, 1996.

838 Foken, T., Göckede, M., Mauder, M., Mahrt, L., Amiro, B. D., and Munger, J. W.:
839 Post-field data quality control, in: *Handbook of micrometeorology: a guide for*
840 *surface flux measurement and analysis*, Lee, X., Massman, W. J., and Law, B.:
841 Kluwer, Dordrecht, 181-208, 2004.

842 Foken, T., Aubinet, M., Finnigan, J. J., Leclerc, M. Y., Mauder, M., Paw, U. K. T.:
843 Results of a panel discussion about the energy balance closure correction for
844 trace gases. *Bull Am. Meteorol. Soc.*, 92(4), ES13-ES18, 2011.

845 Galanti, B. and Tsinober, A.: Is turbulence ergodic? *Physics Letters A*, 330, 173–18,
846 2004.

847 Higgins, C. W., Katul, G. G., Froidevaux, M., Simeonov, V. and Parlange, M. B.:
848 Atmospheric surface layer flows ergodic? *Geophys. Res. Lett.*, 40, 3342-3346,
849 2013.

850 Hu, Y.: Convergence movement influence on the turbulent transportation in
851 atmospheric boundary layer, *Adv. Atmos. Sci.*, **20**(5), 794-798, 2003.

852 Hu, Y., Chen, J., Zuo, H.: Theorem of turbulent intensity and macroscopic mechanism
853 of the turbulence development, *Sci China Ser D-Earth Sci*, **37**(2), 789-800, 2007.

854 Hu, Y., and Chen, J.: Nonequilibrium Thermodynamic Theory of Atmospheric
855 Turbulence, In: *Atmospheric Turbulence, Meteorological Modeling and*
856 *Aerodynamics*, Edited by Peter R. Lang and Frank S., Nova Science Publishers,
857 Inc., 59-110, 2009.

858 Kaimal, J. C. and Wyngaard, J. C.: The Kansas and Minnesota experiments, Bound.

859 Lay. Meteor., 50, 31-47, 1990.

860 Kaimal, J. C. and Gaynor, J. E.: Another look at sonic thermometry, Bound. Lay.
861 Meteor., 56, 401–410, 1991.

862 Katul, G. G., Hsieh, C. I.: A note on the flux-variance similarity relationships for heat
863 and water vapor in the unstable atmospheric surface layer, Bound. Lay. Meteor., 90,
864 327–338, 1999.

865 Katul, G., Cava, D., Poggi, D., Albertson, J., and Mahrt, L.: Stationarity, homogeneity,
866 and ergodicity in canopy turbulence, Handbook of micrometeorology a guide for
867 surface flux measurement and analysis, Lee, X., Kluwer Academic Publishers,
868 New York, 161–180, 2004.

869 Krengel, U.: Ergodic theorems, de Gruyter, Berlin, New York, 363, 1985.

870 Lennaert van, V., Shigeo, K., and Genta, K.: Periodic motion representing isotropic
871 turbulence, Fluid Dyn. Res., 38, 19–46, 2006.

872 Li, X., Hu, F., Pu, Y., Al-Jiboori, M. H., Hu, Z., and Hong, Z.: Identification of
873 coherent structures of turbulence at the atmospheric surface layer, Adv. Atmos.
874 Sci., 19(4), 687-698, 2002.

875 Mauder, M., Desjardins, R. L., MacPherson, J.: Scale analysis of airborne flux
876 measurements over heterogeneous terrain in a boreal ecosystem. J. Geophys. Res.
877 112, D13112, 2007.

878 Martano, P.: Estimation of surface roughness length and displacement height from
879 single-level sonic anemometer data, J. Appl. Meteorol., 39(5), 708–715, 2002.

880 Mattingly, J. C.: On recent progress for the stochastic Navier Stokes equations,
881 Journées équations aux dérivées partielles, Univ. Nantes, Nantes, Exp. No. XI,
882 1-52, 2003.

883 McMillen, R. T.: An eddy correlation technique with extended applicability to non

884 simple terrain, *Bound. Lay. Meteor.*, 43, 231-245, 1988.

885 Moore, C. J.: Frequency response corrections for eddy correlation systems, *Bound.*
886 *Lay. Meteor.*, 37, 17-35, 1986.

887 Neumann, J. V.: Proof of the quasi-ergodic hypothesis, *Mathematics Proc. N. A. S.*,
888 18, 70-82, 1932.

889 Oncley, S. P., Friehe, C. A., John, C. L., Businger, J. A., Itsweire, E. C., Chang, S. S.:
890 Surface-Layer Fluxes, Profiles, and Turbulence Measurements over Uniform
891 Terrain under Near-Neutral Conditions, *J. Atmos. Sci.*, 53 (7), 1029-1044, 1996.

892 Padro, J.: An investigation of flux-variance methods and universal functions applied
893 to three land-use types in unstable conditions, *Bound. Lay. Meteor.*, 66, 413-425,
894 1993.

895 Panofsky, H. A., Lenschow, D. H., and Wyngaard, J. C.: The characteristics of
896 turbulent velocity components in the surface layer under unstable conditions. *Bound.*
897 *Lay. Meteor.*, 11, 355-361, 1977.

898 Papoulis, A. and Pillai, S. U.: Probability, random variables and stochastic processes.
899 McGraw-Hill. New York. 666, 1991.

900 Poulos, G. S., Blumen, W., Fritts, D. C., Lundquist, J. K., Sun, J., Burns, S. P., Nappo,
901 C., Banta, R., Newsom, R., Cuxart, J., Terradellas, E., and Balsley, Ben.: CASES-99:
902 a comprehensive investigation of the stable nocturnal boundary layer. *Bull. Amer.*
903 *Meteor. Soc.*, 83, 555-581, 2002.

904 Schotanus, P., Nieuwstadt, F. T. M., and de Bruin, H. A. R.: Temperature measurement
905 with a sonic anemometer and its application to heat and moisture fluxes, *Bound.*
906 *Lay. Meteor.*, 26, 81-93, 1983.

907 Stull, R. B.: An introduction to boundary layer meteorology. Kluwer Academic Publ.
908 Dordrecht. 670, 1988.

909 Uffink, J.: Boltzmann'S work in statistical physics, Stanford encyclopedia of
910 philosophy, Edward, N. Z., 2004.

911 Vickers, D., Mahrt, L.: Quality control and flux sampling problems for tower and
912 aircraft data. *J. Atmos. Oceanic. Technol.*, 14, 512-526, 1997.

913 Webb, E. K., Pearman, G. I., and Leuning, R.: Correction of the flux measurements for
914 density effects due to heat and water vapor transfer, *Q. J. R. Meteorol. Soc.*, 106,
915 85–100, 1980.

916 Wilczak, J. M., Oncley, S. P., Stage, S. A.: Sonic anemometer tilts correction
917 algorithms. *Bound. Lay. Meteor.*, 99(1), 127-150, 2001.

918 Wyngaard, J. C.: *Turbulence in the atmosphere, getting to know turbulence*,
919 Cambridge University Press, 2010.

920 Zuo, H., Xiao X., Yang Q., Dong L., Chen J., Wang S.: On the atmospheric movement
921 and the imbalance of observed and calculated energy in the surface layer, *Sci. China.*
922 *Ser. D-Earth Sci.*, 55(9), 1518-1532, 2012.

923

924

925
926

Te 1 Local Stability Parameter $(z-d)/L_c$ of the Eddies in Different Temporal Scales on August 25

Time	3:00-4:00	7:00-8:00	14:00-15:00
Eddy scale			
≤ 2 min	0.59	0.52	-0.38
≤ 3 min	0.31	0.38	-0.44
≤ 5 min	0.28	0.16	-0.40
≤ 10 min	-0.01	0.15	-0.34
≤ 30 min	-0.04	-0.43	-0.27
≤ 60 min	-0.07	-1.29	-0.30

927

Te 2 Parameters of the Fitting Curve of MOS relation for Vertical Velocity Variance

	10 min		30 min		60 min	
	$z/L < 0$	$z/L > 0$	$z/L < 0$	$z/L > 0$	$z/L < 0$	$z/L > 0$
c_1	1.08	1.17	1.06	1.12	0.98	1.06
c_2	4.11	3.67	3.64	3.27	4.62	2.62
R	0.97	0.76	0.94	0.56	0.83	0.30
S	0.19	0.25	0.17	0.27	0.25	0.31

928

929

930

931

932

933

934

935

936

937

938

939

940

941

942

943

944

945

946

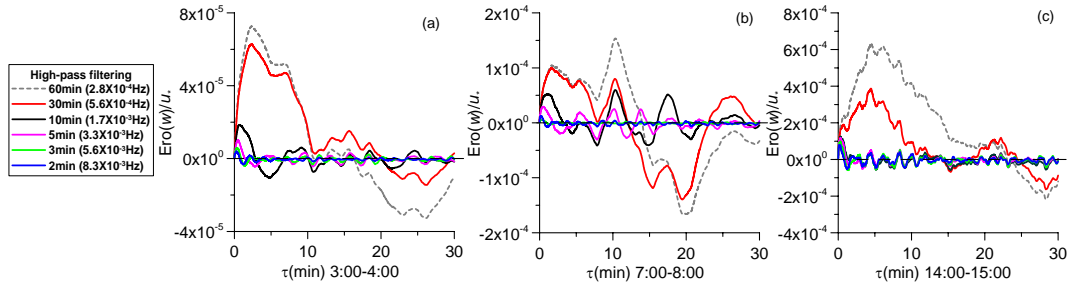
947

948

949

950

951



952

953

954

955

956

957

Fig. 1. Variation of mean ergodic function $Ero(w)$ of vertical velocity measured at the height 3.08 m in NSPCE with relaxation time for the different scale eddies after High-pass filtering. Panels (a), (b) and (c) are the respective results of the three time frames. If their mean ergodic function is more approximate to zero, then the average of eddies in the corresponding temporal scale will more closely satisfy the ergodic conditions.

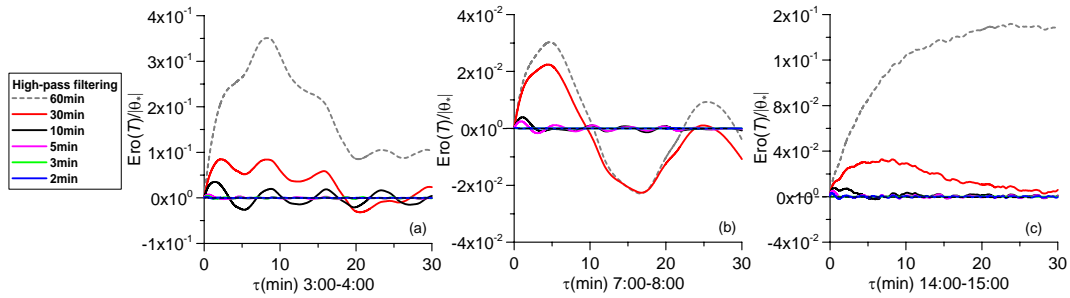
958

959

960

961

962



963

964

965

966

967

968

Fig. 2. Variation of mean ergodic function $Ero(T)$ of the different scale eddies of temperature with relaxation time (other conditions are similar to Fig. 2, and the same applies to the following figures).

969

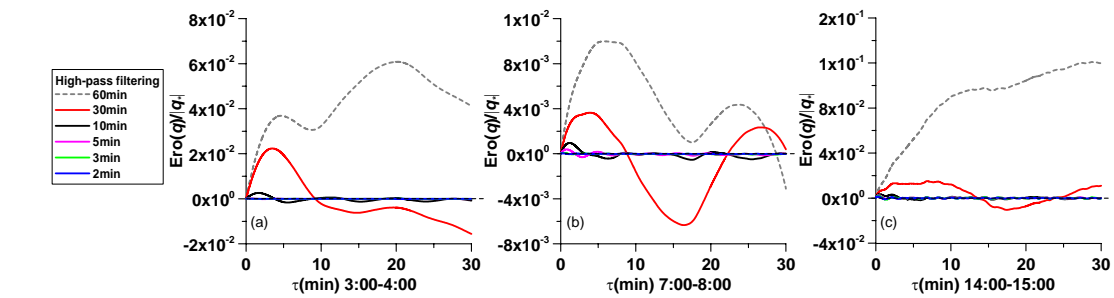
970

971

972

973

974



975

976

Fig. 3. Variation of mean ergodic function $Ero(q)$ of the different scale eddies of humidity with relaxation time.

977

978

979

980

981

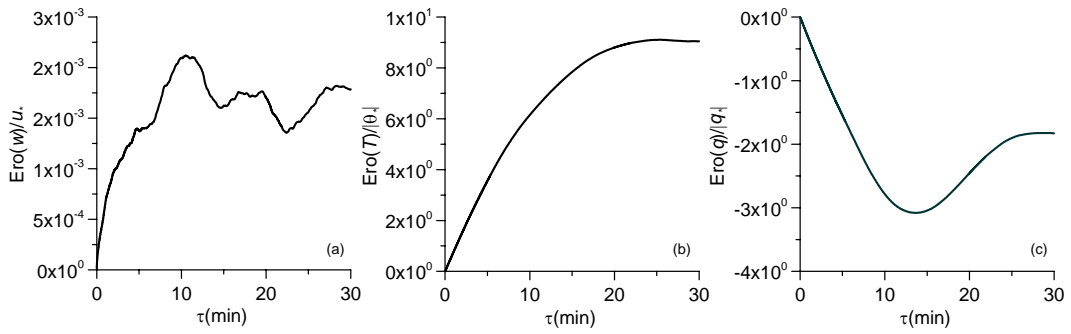
982

983

984

985

986



987 Fig. 4. Variation of mean ergodic function $Ero(w)$ of the vertical velocity (a), temperature (b) and specific humidity (c) before filtering during midday 14:00-15:00 (CST) in NSPCE with relaxation time τ .

988

989

990

991

992

993

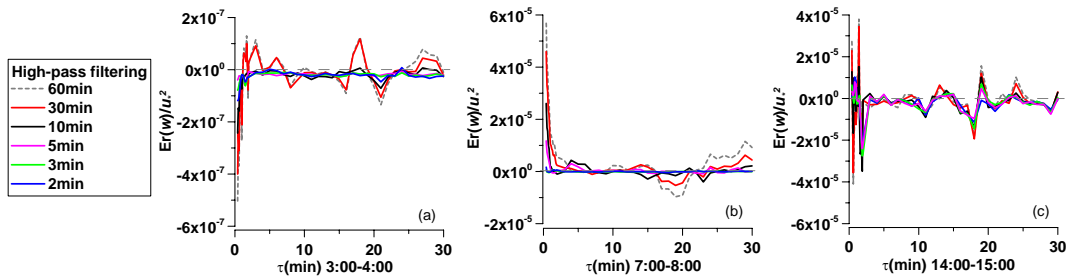
994

995

996

997

998



999 Fig. 5. Variation of the autocorrelation ergodic function of vertical velocity with relaxation time for different scale eddies.

1000

1001

1002

1003

1004

1005

1006

1007

1008

1009

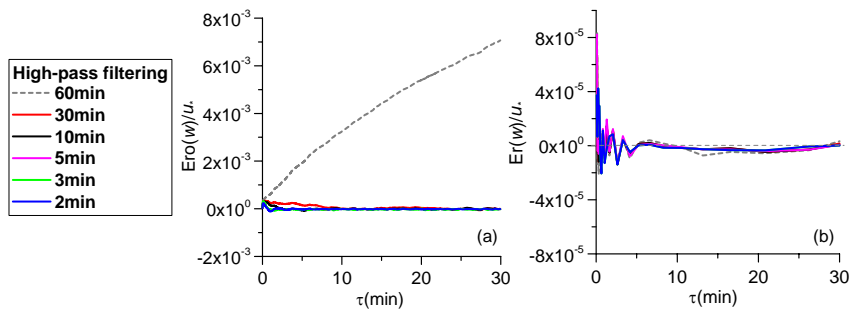


Fig. 6. Variation of mean ergodic function (a) and autocorrelation ergodic function (b) of the vertical velocity with relaxation time for the different scale eddies in CASES-99's seven stations.

1010
 1011
 1012
 1013
 1014

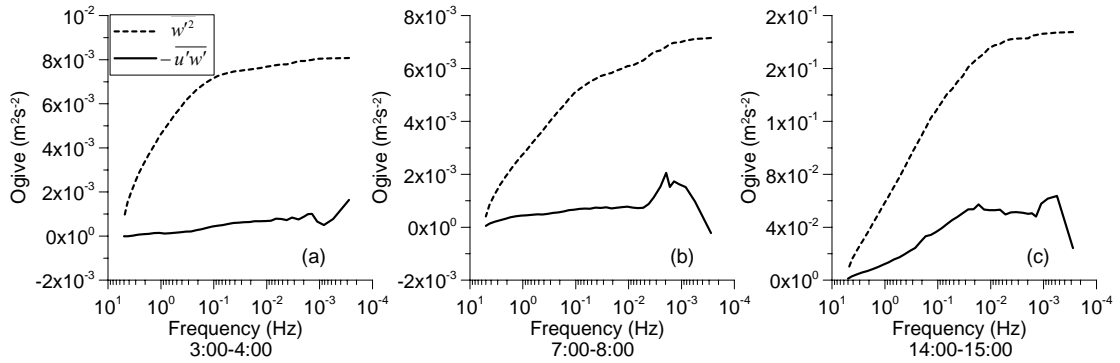


Fig. 7. Variation of Ogive functions of $\overline{w'^2}$ and $-\overline{u'w'}$ with frequency at the height 3.08 m in NSPCE for the three time frames.

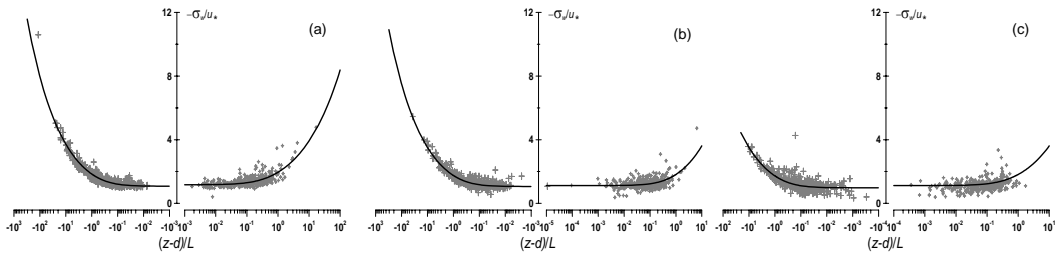


Figure 8. MOS relation of vertical velocity variances of the different scale eddies in NSPCE; Panels (a), (b) and (c) respectively represent the similarity of eddies of 10 min, 30 min and 60 min in the temporal scale.

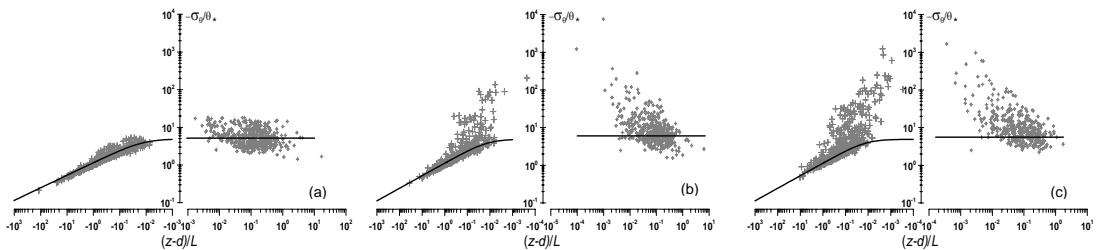


Figure 9. MOS relations of temperature variance of in different scale eddies of NSPCE; Panels (a), (b) and (c) respectively represent the similarity of the eddies of 10 min, 30 min and 60 min in the temporal scale.